

Supplementary Information

Metal-Insulator-Metal waveguides via angled metal deposition for particle manipulation and separation by size

Saara A. Khan^{1*}, Chia-Ming Chang², Zain Zaidi¹, Wonseok Shin¹, Yu Shi¹, Audrey K. Ellerbee Bowden¹, and Olav Solgaard¹

¹Stanford University, Department of Electrical Engineering, Stanford, California 94305

²Bell Labs, Alcatel-Lucent, 791 Holmdel Road, Holmdel, New Jersey 07733, USA

*saarak@stanford.edu

1. Simulation Method

The evanescent field from a MIM waveguide exerts an optical gradient and propulsion forces that trap and propagate particles located near the evanescent field of the waveguide. The optical force can be computed numerically using COMSOL from the geometry and particle size. We use a similar simulation space as previously reported.¹ The dimensions for the Au-Si₃N₄-Au waveguide were 300-nm tall, 400-nm wide, and 50-nm gold sidewalls; and the dimensions for the Au-H₂O-Au waveguide were 300-nm-tall gold sidewalls, 50-nm gold sidewalls, and a 10- μ m gap filled with water (the surrounding region is also covered with water). For the simulation, we tuned our input light polarization to be TM and at a wavelength of 1550 nm. For material properties, we assume a silicon nitride waveguide (2.09) with silica as the under cladding (1.5) and water as the upper cladding (1.33). The refractive index for gold at 1.5 μ m was chosen to be 0.55 (real) and 9.53 (imaginary part). We model homogeneous silicon dioxide particles (1.5). We assume a 10-nm gap spacing between the particle and the waveguide top-surface as in our previous models¹.

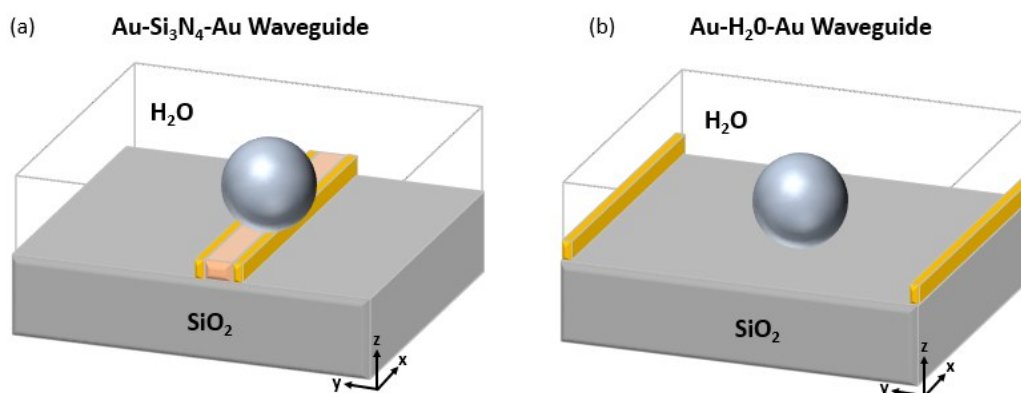


Figure S 1: COMSOL schematics (a) MIM1, (b) MIM2

The optical gradient and propulsion forces at 2- μ m from the entrance of the waveguide for the Au-Si₃N₄-Au (Fig S1a) and Au-H₂O-Au waveguides (Fig S1b) are shown in Table 1 and Table 2.

Diameter	Propulsion Force (F_x)	Gradient Force (F_z)
1.0 μm	2.6e-9 pN/W	-8.45e-10 pN/W
2.0 μm	6.1e-10 pN/W	-10.1e-10 pN/W
3.0 μm	4.88e-10 pN/W	-11.6e-9 pN/W
4.0 μm	3.73e-10 pN/W	-14.8e-9 pN/W

Table 1: Au-Si₃N₄-Au Waveguide

Diameter	Propulsion Force (F_x)	Gradient Force (F_z)
1.0 μm	4.133e-12 pN/W	-3.926e-12 pN/W
2.0 μm	4.269e-11 pN/W	-1.826e-12 pN/W
3.0 μm	8.75e-11 pN/W	-1.35e-11 pN/W
4.0 μm	2.5e-10 pN/W	-1.65e-10 pN/W

Table 2: Au-H₂O-Au Waveguide

The optical gradient and propulsion forces decay as a result of the attenuation of the guided modes inside the waveguide. We obtained the propagation distance of the Au-Si₃N₄-Au waveguide by solving the waveguide mode equation for the two lowest-order modes for individual wavelengths separated by 50-nm between 800-nm and 1800-nm using an open-source finite-difference frequency-domain solver². The dispersion relation confirms that Mode 1 ($L_{p1} = 18.9\text{-}\mu\text{m}$) is the fundamental mode and Mode 2 ($L_{p2} = 14.2\text{-}\mu\text{m}$) is the second-order mode of the wavelength.

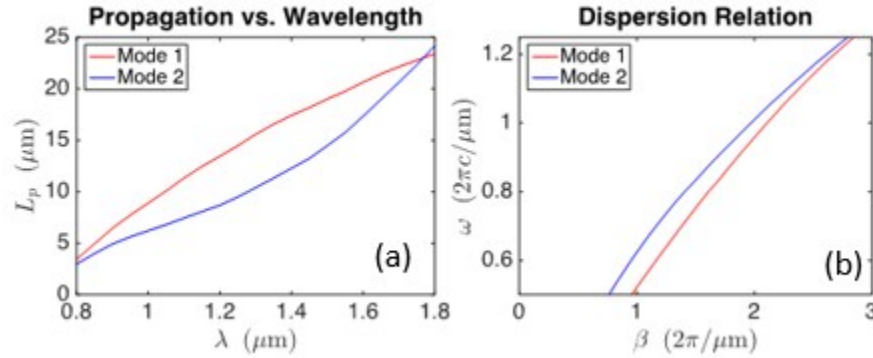
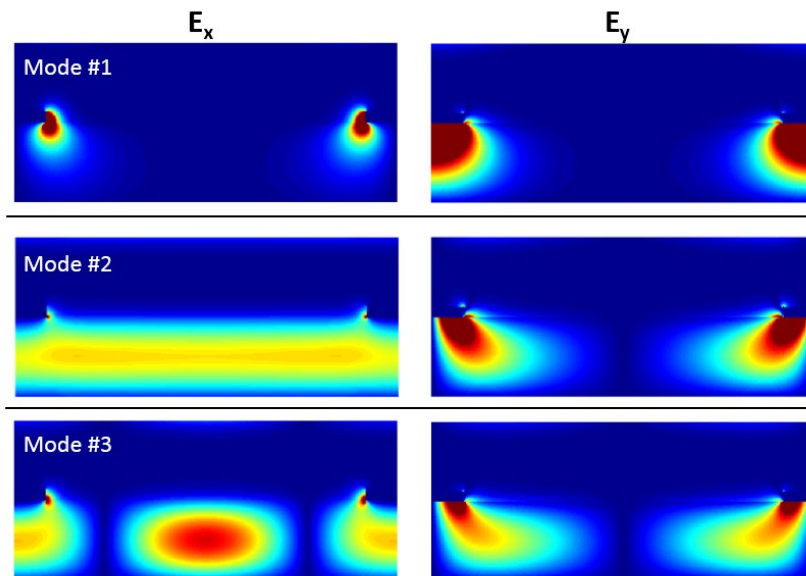


Figure S 2: (a) Propagation distance L_p as a function of wavelength and (b) the dispersion relation of Mode 1 and Mode 2

We have calculated the modes of the outer waveguide using 2-D FDTD to model the cross-section of the Au-H₂O-Au waveguide shown in Fig S1(b) with a periodic boundary condition. The propagation length of the first mode of the waveguide is 0.190 mm (plasmonic mode) and the two higher order modes are unguided modes in the SiO₂. The unguided modes in the SiO₂ interact with the gold sidewalls to create an electric field and also generate an evanescent field in the water region of the device. To address limitations in 2-D simulations from solving for the propagation distance of the unguided modes, we used a 3-D simulation in COMSOL to find the propagation length of the superposition of the many non-confined outer waveguide modes to be 1.88-mm. Experimentally we found the decay length of the outer waveguide to be 1.8 mm (L_{p3}),

which takes the non-confined outer waveguide modes into account. We have used the experimental decay length of the outer waveguide in our model as it reflects most accurately the combined multimodal coupling effect.

Figure S 3: 2-D FDTD simulations of the outer waveguide structure. The device is highly multimodal and the first three modes are shown. The first mode is a plasmonic mode and has a decay length of 0.19 mm. The second and third modes are unguided modes in the SiO₂.



2. Fabrication Methodology

The Innotec ES26C e-beam evaporator and the Metalica sputter systems in the Stanford Nanofabrication Facility (SNF) were used for depositing and comparing sidewall metal coverage. We compared the e-beam evaporator to the metal sputtering technique and found the angled e-beam evaporator to have more uniform sidewall coverage than sputtering as shown in Fig S4.

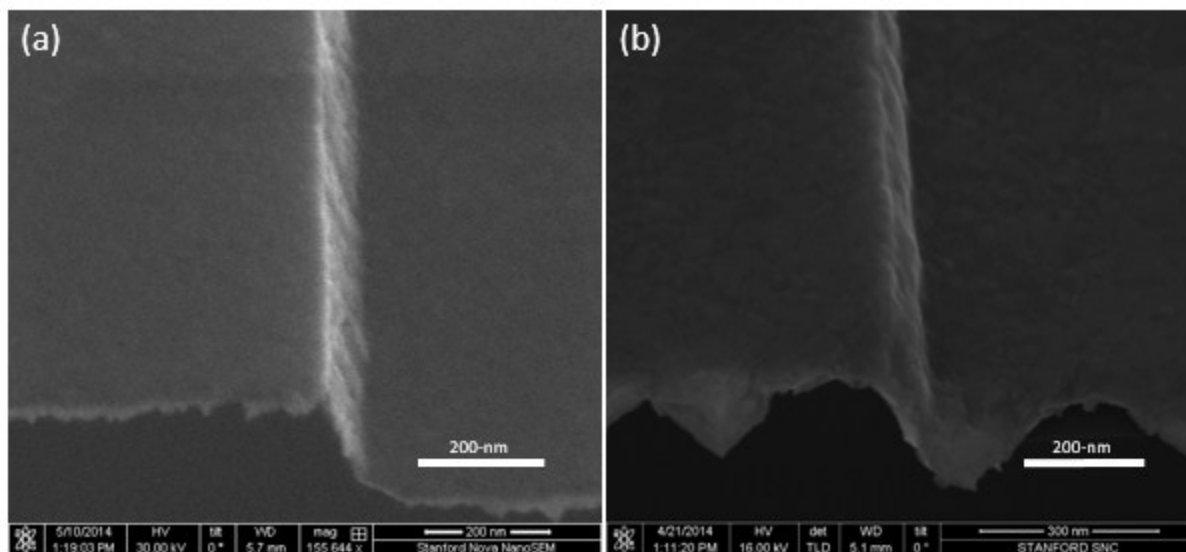


Figure S 4: An SEM image of the device after deposition of RF sputtering (a) and double angled sidewall metal deposition via electron beam deposition (b). Gold covers the top of the device and the sidewalls. It can be seen that gold sidewall deposition from RF sputtering is patchy compared to double angled sidewall deposition from electron beam deposition. Difference in contrast between the two images is due to differences in kV used to image the device (30 kV for (a) and 16 kV for (b)).

After depositing metal through e-beam evaporation, we then etched our samples to remove metal on horizontal surfaces. We conducted a directional Argon sputter etching to remove gold on all surfaces with the exception of gold on the sidewalls of the channel waveguides.

We used a plasma reactive ion etching system to perform the Argon sputter etching. We varied specific parameters (etch time, RF power, chamber pressure, Argon flow) to understand which parameter changes would obtain optimal surface etching. For single-angled deposition for 50-nm of gold, we performed several parameter iterations to find optimal sidewall coverage. Standard recipes suggest Ar gas flow rate at 15-sccm, chamber pressure 12-mT, RF power at 100W, and peak voltage at 660V for a gold etch of 90Å/min in the MRC Model 55 RIE. We initially used these parameters and found the high etch rate led to samples being non-directionally etched. We found that at a RF power of 70W we had better control over various etch times to find optimal timing for sidewall etch control. At 70W, we varied etch times between 180-300 seconds. Etch times below 220 seconds still exhibited gold on the surface. Times above 230 seconds looked completely etched from a 50x objective in a standard microscope. However, from SEM images we found that times under 290 seconds still contained a thin nanolayer of gold on the surface as shown in Fig S5.

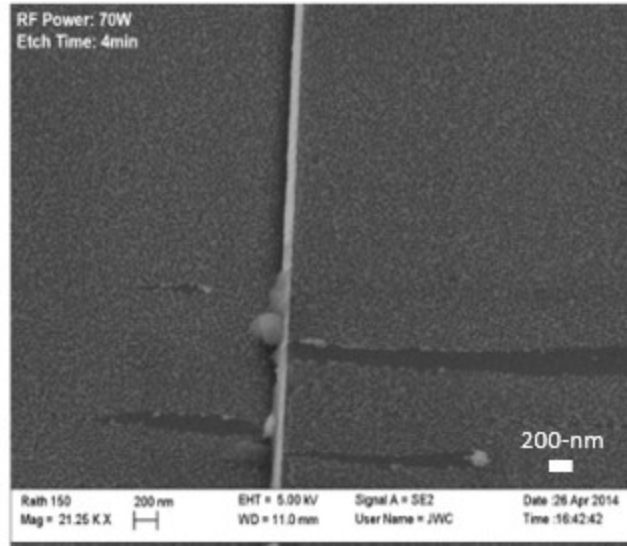


Figure S 5: SEM image from conducting Argon etching for 4 minutes. A thin nanolayer of gold is still on the surface and has not been completely removed.

We found that at 300 seconds the gold film had been completely removed from the surface and a robust sidewall of gold has been deposited on the waveguide. Once this time was found for an e-beam angled deposition of 50-nm, it was found to be repeatable within ± 5 seconds with the same chamber conditions. The repeatability time frame can vary with a shared facility due to the high influx of users using various gases in the chamber and can extend variability up ± 100 seconds if the system is not thoroughly purged. However, this procedure does provide a robust technique that one can implement to find the right etch time for different instruments and achieve sidewall metal deposition.

Using the procedure detailed, we implemented a double-angled sidewall metal deposition on silicon nitride waveguides to coat gold on both sidewalls of the waveguide. For a double-angled deposition, the etch times were twice that of the single-angled deposition. The system parameters were the same as single-angled deposition with an Argon flow rate of 15-sccm, RF power 70W, and chamber pressure of 12-mT. Images of the final device can be found in the main text in Fig 6b and Fig 7a.

3. Particle Trapping

Silicon dioxide particles (size range 2-10 μm) were suspended in distilled water and injected to the beginning of the waveguide entrance. The particles were trapped once within proximity (7-10 μm) of the guide as shown in Fig S6.

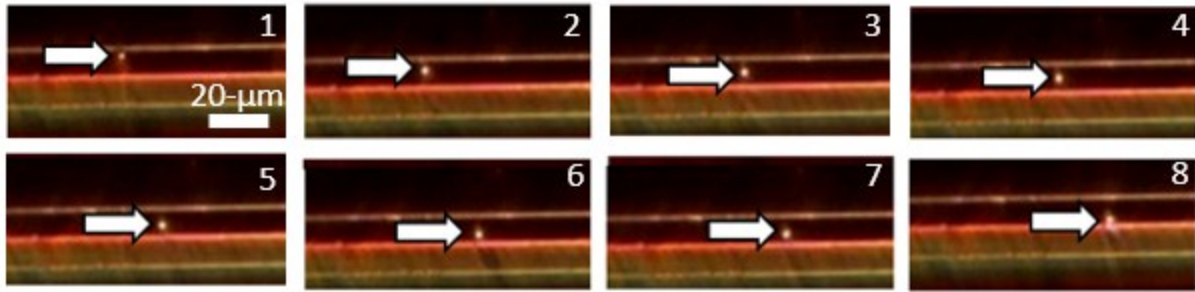


Figure S 6: Sequence showing the trapping of a glass particle within 7-10- μm proximity of the inner waveguide

References

- 1 S. A. Khan, Y. Shi, C.-M. Chang, C. Jan, S. Fan, A. K. Ellerbee and O. Solgaard, *Opt. Express*, 2015, **23**, 8855.
- 2 W. Shin, 2015. <https://github.com/wsshin/maxwellfdfd>